

Multi Sensor Image Matching using Super Symmetric Affinity Tensors based HyperGraph Matching



Hari Prasada Raju Kunadharaju, N. Sandhya, Raghav Mehra

Abstract: Image Matching technique is regularly on one of the main errands in numerous Photogrammetry and Remote Sensing applications. Based on multi-discipline, the approach of multiple sensor image matching is a novel one established which has vital application in military, civil, medicinal, and certain other domains. However, image matching approach faces numerous challenges, specifically in multi-sensor images where the images are gathered from the different sensor with different intensities, scales, and moments. Thus, a novel image matching approach is introduced in this paper using affinity tensor and HyperGraph Matching (HGM) technique that attempts to overcome certain drawbacks in matching and increases performance accuracy. Hypergraph matching techniques are employed using affinity tensors and consider supersymmetric property during construction. Graphs are constructed using graph theory for both sources, and target image and matching is done using third-order tensors. The experimental outcomes displayed that the proposed technique has good recall, precision, and positive accuracy values compared to the existing two descriptors based and tensor-based matching algorithms.

Keywords: Multi Sensor Images; Image matching; Super Symmetric; Affinity Tensor; Graph Matching; Third Order

I. INTRODUCTION

At present, we are living in the “golden era of Earth observation,” categorized through numerous aerial and space-borne sensors giving an extensive assortment of remote sensing information. In this case, each sensor owns diverse individualities, aimed for a particular job. The technique of multiple sensor image matching is a novel approach introduced. Based on multi-discipline, the technology of multi-sensor image matching is a new technology established which has significant application in military, civil, medical, and certain other domains[1]. The problems the image matching methodology is to the imaging mechanism is dissimilar, the gray correlation is smaller, and there are numerous dissimilarities amongst the images like scalability, viewer angle, illumination, resolution, etc. [2].

Revised Manuscript Received on 30 July 2019.

* Correspondence Author

Hari Prasada Raju Kunadharaju*, Research scholar from Bhagwant University, Ajmer Vice-President, Wells Fargo Enterprise Global Services
N. Sandhya, Professor, Department of Computer Science & Engineering, VNR Vignana Jyothi Institute of Engineering & Technology
Raghav Mehra, Associate Professor, Department of Computer Science & Engineering, Bhagwant University Ajmer

© The Authors. Published by Blue Eyes Intelligence Engineering and Sciences Publication (BEIESP). This is an [open access](https://creativecommons.org/licenses/by-nc-nd/4.0/) article under the CC-BY-NC-ND license <http://creativecommons.org/licenses/by-nc-nd/4.0/>

For many applications, the matching of multi-sensor images is significant preprocessing step, such as data-fusion, navigation, and visualization tasks. Due to different physical characteristics of different sensors, the association between the intensities of the matching pixels is multifaceted. The presence of Visualfeatures in one sensor image may not seem to be another one, and vice versa. In the same regions, Image contrast may differ from each other, multiple intensities in one image might be plotted to a single intensity in other images, and vice versa. The uncorrelated intensities make the normal intensity-based matching methods ineffective. Therefore, the matching of the multi-sensor image becomes challenging in computer vision.

Comparing multiple sensor images are an inspiring task because of textual variations and non-linear variances. There are two reasons for challenging in matching. Originally, images of similar scenes using diverse sensors frequently have diverse radiometric features known as nonlinear intensity variances. Due to this difference caused by various sensor and illumination, the distance between characteristics points is not nearby, leading to an incorrect match. Secondly, images from diverse sensors are frequently taken at diverse moments that lead to substantial textural variations. Both these issues cause less matching accuracy and unsatisfying matching results.

Therefore, a novel image matching approach is suggested in this paper for multi-sensor images by affinity tensor and HyperGraph Matching (HGM) technique. To significantly progress the matching performance, graduated projection of constant solution to the distinct fields suggested on affinity tensor. The HGM approach is employed to match different sensor images using finding an optimum group of vertex assignments for the two graphs constructed using source and target images. The graph matching is accomplished by using third-order affinity tensor that increases the dimension of the feature points. Thus, the symmetric property is used, which is invariant under any permutation of its indices and constructs supersymmetric affinity tensor and updates using the probabilistic values for graph matching.

II. LITERATURE SURVEY

Lately, various analysts at home and abroad have finished an extensive proportion of investigation in the domain of multiple sensor image matching [3, 4, 5]. Remote sensing is coordinating and combination of multi-sensor information. Discovering consistent and dependable characteristics in various information source is a troublesome undertaking.



Past approaches such as [6], demonstrating auspicious outcomes relating to the issue of optical and SAR image coordinating using layouts. The downside of these layout-aided methodologies is the requirement for extricating an appropriate characteristic.

SAR-SIFT is an effective method which was proposed [7] and the original grayscale dissimilarities aided gradient operations was substituted using a ratio-aided gradient operation. This contribution assists SAR-SIFT strong to SAR noise and performs better matching. In SAR-SIFT, issues are yet present. Initially, the rectangular bi-windows are received in the radio-aided gradient operation. This generates undesirable higher frequency reactions round genuine characteristics and influences the consistency of the strategy. Secondly, SAR-SIFT is intended to deal speckle noise in SAR images yet do not take into account non-direct grayscale contrast among SAR and optical images. Hence, this strategy can't get palatable outcomes for image matching.

The other sort of methodologies dependent on shape features is suggested [8– 10] by utilizing nearby self-similitude [11] or phase congruency [12,13] to develop feature descriptor. This sort of descriptors could catch neighborhood geometric features of an image and is vigorous to image grayscale alterations. This noise in the SAR picture isn't measured in any case in these techniques. They are region-based coordinating techniques which are delicate to geometric image falsification. Line features are likewise employed to coordinate SAR and optical images [14]

A strong feature descriptor depending on Gaussian-Gamma-shaped (GGs)bi-windows [15] is built, and a whole architecture for image matching is suggested. Merely, the matching performance cannot be improved by suggestively enhancing the feature identifier, descriptor merely, or matching criterion, however, intended on improving the complete matching efficiency via enhancing the strategy and certain phases in the workflow To compare multimodal images, in [16] suggested developing phase congruency as a simplification of gradient data. The method presented in [17] outspreads this usage of phase congruency to generate a radiation-invariant characteristics transformation, i.e., lesser vulnerable to nonlinear radiation misrepresentations.

The usage of a Siamese CNN framework and to figure comparative change amongst SAR and optical image patches were proposed by Merkle et al. [18], with the aim of enlightening geo-localization accurateness of optical images. In [19], the usage of a pseudo-Siamese CNN is suggested framing SAR-optical communication issue as binary categorization. They generate proof with this approach to the applicability of CNN's for comparing diverse remote sensing images. By the altered fusion layer and softmax loss function, Hughes et al. [20] prolonged this primary investigation as to evaluate a similarity possibility score. Moreover, the research was prolonged to pretend a practical feature matching situation and was capable of attain around 86% accurateness using an 11% false-positive rate (FPR).

As radiometric and geometric data of image features could be effectively encrypted in tensor, the affinity tensor amongst graphs named as the core of graph matching [21], covers the manner for which multi-sensor image matching. In feature matching, [22] employed geometric constraints and added satisfactory matching outcomes. Based on a multi-tensor, Wang et al. [23] projected a new matching method which will

merge multiple granularity geometric affinity. From this, the experimental outcomes exhibited the methodology is having further strong compared to the methodology suggested in [22]. In [24, 28], a weighted affinity tensor is suggested for poor texture image matching and improved experimental outcomes associated with the feature-aided matching approach as it witnessed that outliers are unavoidable in comparison.

III. PROBABILISTIC HYPERGRAPH IMAGE MATCHING USING SUPER SYMMETRIC AFFINITY TENSORS

In this section, a novel image matching methodology is suggested for multi-sensor images to obtain the corresponding characteristics employing super matching tensor technique which incorporates geometric and radiometric data. The target and source images given using diverse sensors are employed to find the feature point correspondence amongst the two images. This process comprises of two dissimilar phases to obtain the matching amongst the images. They are:

III. I Construction of complete graph from sensor images

Let F_S and F_T denotes the features points mined from source and target image with m and n a number of features, correspondingly. $i(i < m)$ and $i'(i' < n)$ denotes to feature indices of F_S and F_T . The whole graphs are constructed for the two images as given in [32] referred to as G_S and G_T . In the arithmetical domain of graph theory, the whole graph is a flexible undirected graph where each group of dissimilar nodes is linked using a unique edge.

Problem Formulation:

A hypergraph $G = \{V, L, E, W\}$ of dimension M is given using the vertex group $V = \{1, \dots, M\}$, a vertex label group $L = \{l_1, \dots, l_M\}$, a finite hyper-edge set $E = \{e_1, e_2, \dots\}$, and a finite hyper-edge weight group $W = \{w_{e_1}, w_{e_2}, \dots\}$. A vertex label $l_i \in R_1^D$ denotes to the descriptor vector for the vertex. Unlike from the normal graph edge $e = ij$ that links two vertices i and j , a hyper-edge $e_1 = ij \dots$ can link numerous vertices.

In this paper, the concentration is merely on 3-uniform hypergraph, deprived of considering the pairwise and high-order relationship. Thus, hyper-edge $e_1 = ijk$ is a triad, and hyper-edge weight $w_{ijk} \in R_w^D$ is a vector defining the structure behavior of triad k . Specified two hypergraphs G of dimension M and H dimension, a similarity amongst them is to evaluate an optimum group of assignments amongst the two vertex groups V_G and V_H . Arithmetically, these assignments could be denoted using the assignment matrix $\in \{0, 1\}^{M \times N}$. Precisely, $X_{i,p} = 1$ signifies that there persist an assignment $\{i, p\}$ amongst vertex i in G and p in H , and $X_{i,p} = 0$ refers that none of the assignments persists amongst two vertices.

The resemblance amongst G and H could be encrypted using the non-negative third-order tensor $A \in [0, +\infty)^{M \times M \times M \times M \times M}$ given using the affinity tensor that is a 3-way array and simplification of affinity matrix in pairwise graph matching approach [25, 26]. It is a tensor entity present in column I, row J, cube k. To clearly define the way the tensor entities rebuild, (i, i') , (j, j') and (k, k') are employed to replace $I, J, \text{ and } K$. The indices $i, j, \text{ and } k$ are feature

elements in source image varying from 0 to $m - 1$ and i', j', k' are feature elements in target image varying from 0 to $n - 1$. Thus, the tensor element $a_{i,l,k}$ is rewritten as $a_{i,i',j,j';k,k'}$ located at $(i \times n + i')$ column, $(j \times n + j')$ row, and $(k \times n + k')$ tube, and it states the resemblance of triangles, which are two triangles in graph respectively.

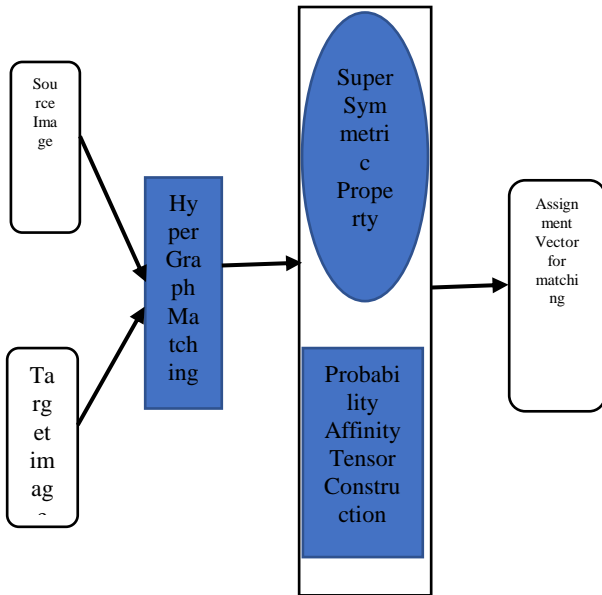


Fig 1: Block Diagram for the Proposed Approach

III.II HyperGraph Matching Approach

HyperGraph Matching (HGM) is an essential issue that intends to obtain an optimum group of vertex assignment amongst graphs that searches for the higher-order relationship amongst vertices away from pairwise indications. The HGM is performed through presenting affinity tensor updating using graduated projection. This issue is initially articulated as the combinatorial optimization issue in higher-order polynomial, which is undisturbed and inferred in a probabilistic way and is almost resolved using the iterative approach. The update of affinity tensor in every iteration is accomplished by encoding high-order similarity between hypergraphs, apart from the update of the probabilistic assignment vector. Thus, the ultimate assignment vector attained is frequently very adjacent to a distinct field.

The tensor element $a_{i,i',j,j';k,k'}$ could be evaluated through

$$(1):$$

$$a_{i,i',j,j';k,k'} = \begin{cases} e^{-\frac{(w_b \cdot \|f_{i,j,k} - f_{i',j',k'}\|_2)^2}{\epsilon^2}} & \text{if } i = j = k \text{ and } i' = j' = k' \\ e^{-\frac{\|f_{i,j,k} - f_{i',j',k'}\|_2^2}{\epsilon^2}} & \text{if } i \neq j \neq k \text{ and } i' \neq j' \neq k' \\ 0 & \text{others} \end{cases} \quad (1)$$

Where $f_{i,j,k}$ and $f_{i',j',k'}$ are geometric descriptors of $T_{i,j,k}^S$ and $T_{i',j',k'}^T$. These descriptors are typically conveyed as the cosines of three vertical angles in a triangle such as $f_{i,j,k} = (\cos\theta_i, \cos\theta_j, \cos\theta_k)$. The variable ϵ signified Gaussian kernel bandwidth. $\|\cdot\|$ is w_b a balanced factor which will be given as $w_b = \frac{\bar{f}_r}{\bar{f}_a}$ where \bar{f}_r and \bar{f}_a are

average distances of radiometric and geometric descriptors correspondingly. Cosine of angles are linked by the geometric descriptors and intensity of image pixels are linked by radiometric descriptors. Both forms of descriptors have diverse physical size. Additionally, the radiometric descriptors are further distinguishing compared to geometric descriptors as radiometric descriptors have a larger size compared to geometric descriptors.

Supersymmetric Affinity Tensor:

The amount of storage needed can be reduced for third-order by considering supersymmetric affinity tensor. A tensor is supersymmetric if its items are invariant beneath any permutation of its indices [23]. A 3rd order supersymmetric tensor T fulfills the relationships:

$$T(i; j; k) = T(i; j; k) = T(i; j; k) = T(i; j; k) = T(i; j; k) = T(i; j; k) \quad (2)$$

Given two feature sets F_S and F_T , with m and n features correspondingly, the supersymmetric affinity tensor is an 3rd order i, j, k , non-negative tensor T_3 , for which a group of indices θ_3 persists, and an 3rd order potential function Φ_3 , where

$$T_3(i, j, k) = \begin{cases} \Phi_3(\Omega(i, j, k)), & \forall (i, j, k) \in \theta_3 \\ 0 & \forall (i, j, k) \notin \theta_3 \end{cases} \quad (3)$$

Where Ω represents random permutation of the vector. A tensor entity using $(i, j, k) \in \theta_3$ is known as a potential element, where other elements are known as zero elements. The potential element refers to a single comparison outcome out of entire probable matching candidates. The amount of storage needed can be reduced by signifying each potential element $T(i, j, k)$ using its canonical entry $T_3(\text{sort}(i, j, k))$. Every stored value hence gives the values of $N!$ elements. Moreover, as zero elements are continuously zero, it is not essential to store them. This significantly diminishes the storage.

HyperGraph Matching using probabilistic affinity tensor:

To make hypergraph matching defined in a probabilistic way, every assignment $\{i, p\}$ could be related using the possibility $P(\{i, a\})$. Consistent with the assignment matrix, the matrix $P \in [0, 1]^{M \times N}$ is a group of assignment possibilities, i.e., $P_{i,p} = P(\{i, p\})$. The affinity tensor is employed to build conditional probability $P(\{i, p\}|\{j, q\}, \{k, r\})$ by a certain function $F(\cdot)$ as

$$Q = F(A) \quad (4)$$

Here Q refers to the group of conditional probability, i.e.

$$Q_{i',j',k'} = Q_{(i-1)N+a, (j-1)N+b, (k-1)N+c} = P(\{i, a\}|\{j, b\}|\{k, c\}) \quad (5)$$

As affinity measures are considering the triad affinity $A(w_{ijk}, w_{abc})$, for example, could be deliberated as the correlation confidence amongst assignments $\{i, p\}$, $\{j, q\}$, and $\{k, r\}$, a directly a mode to attain the conditional probability is:

$$P(\{i, p\}|\{j, q\}|\{k, r\}) = \frac{A_{(i-1)N+p, (j-1)N+q, (k-1)N+r}}{\sum_{j,k,p,q} A_{(i-1)N+p, (j-1)N+q, (k-1)N+r}} \quad (6)$$

Thus a feasible $F(\cdot)$ takes the following form:

$$Q_{i',j',k'} = \frac{A_{i',j',k'}}{\sum_{i',j',k'} A_{i',j',k'}} \quad (7)$$

One foremost issue in this transformation function is affinity behavior in A could be conserved in Q . Consequently, to resolve this issue in tensor condition, affinity conserving arbitrary walk in the pairwise procedure is generalized, whose key notion is to accumulate a fascinating phase in the arbitrary walk. Precisely, the enhanced $F(\cdot)$ considers the below form:

$$Q_{i',j',k'} = \frac{A_{i',j',k'}}{a_{max}} \quad (7)$$

Where $d_{max} = \max_{i,j,k} \sum_{j'} \sum_{k'} A_{i',j',k'}$

Depending on the above description of the assignment $P(\{i, a\})$ and conditional probability $P(\{i, p\}|\{j, q\}, \{k, r\})$, the static assignment probability could be attained using repetitive updating.

$$P^{t+1}(\{i, p\}) = \sum_{j,q} \sum_{k,r} P_t(\{i, p\}|\{j, q\}, \{k, r\}) P_t(\{j, q\}) P_t(\{k, r\}) \quad (8)$$

till its convergence, i.e. $P^{t+1}(\{i, a\}) = P^t(\{i, a\})$.

In the tensor form, (8) could be rewritten as

$$p^{t+1} = Q^t \times_i p^t \times_k p^t, \quad (9)$$

That is precisely the higher-order power iteration. So, every iteration after using (9) the one-to-one constriction of p do not preserve, the Sinkhorn's methodology [27] is used to p^{t+1} , as given in Algorithm.

Probabilistic hypergraph matching algorithm

Input: Two hypergraphs G and H .

Initialize the assignment probability vector $p^0 = \frac{1_{MN}}{N}$

Initialize the weight parameter α

Construct the affinity tensor A by (1) and Q^0 by (7)

repeat

 Update p^{t+1} based on Q^t and p^t by (14),

Repeat

$$P_{(i-1)N+a}^{t+1} = \frac{P_{(i-1)N+a}^{t+1}}{\sum_{i=1}^M P_{(i-1)N+a}^{t+1}}$$

Until convergence

 Update Q^{t+1} , i.e.

$$Q_{i',j',k'}^{t+1} = Q_{i',j',k'}^t \frac{p_{i'}^{t+1} p_{j'}^{t+1} p_{k'}^{t+1}}{p_{i'}^t p_{j'}^t p_{k'}^t}$$

until $P^{t+1} = P^t$

Project P^{t+1} D to get the assignment vector x

Output: An assignment vector x

IV. EXPERIMENTAL RESULTS

Using ZY-3 nadir (ZY3-NAD), ZY-3backward (ZY3-BWD), GF-2, unmanned aerial vehicle (UAV) platform, Jilin1 (JL1) sensors, the suggested Supersymmetric affinity Tensor based HyperGraph Matching (ST-HGM) was assessed using three pairs of images that are seized. To scrutinize its efficiency, two descriptor-aided and one affinity tensor-based matching algorithms are chosen for comparing against proposed ST-HGM approach such as OR-SIFT, GOM-SIFT, and ATBM. These matching approaches were existing in

comparison to multi-sensor images. The comparison for these approaches are ANN algorithm, and the Nearest Neighbor Distance Ratio (NNDR) threshold is to 0.8.

IV. I Evaluation Criterion and Dataset

To, assess the suggested approach, two mutual strategies comprising recall and precision are employed[29,30,31]. The strategies are specified as:

$$recall = CM/C$$

$$precision = CM/M,$$

Here CM refers correct matches which are the count of acceptably matched point pairs, C refers to the correspondences, i.e., the complete count of prevailing correspondences in preliminary feature point group and M refers matches, count of matched points. Along with recall and precision, positional accuracy is also employed to assess the matching efficiency of the proposed approach with the other three approaches. Positional accuracy was evaluated using the root mean square error (RMSE) that was calculated using the affine transformation of the CPs. The dataset description is given in Table 1.

Table 1: Sensor Image Data Samples from Different Sensor

No	Platform	Image Size (Pixels)	Pixel Size (m/Pixel)
1.	GF-2, ZY-3	9376x9136; 24530x24575	1.0, 2.1
2.	ZY3-BWD, ZY3-NAD	24525x24419; 16292x16348	2.1, 3.5
3.	UAV, JL1	4990x3905; 4765x4070	0.5, 1.0

V. RESULTS ANALYSIS

In the feature mining process, UR-FAST is performed in source image; standard FAST is performed in the target image. In the evaluation of affinity tensor, to assurance the iterative rate of image attributes, it obtained 50 UR-FAST attributes in the source image. OR-SIFT, GOM-SIFT, and ATBM were likewise estimated using the test data listed in Table 1.

The measurable description of ST-HGM is briefly mentioned in Fig 2, Fig 3, Fig 3, Fig 4, and matching of the three feature descriptors. ST-HGM outstripped the other three comparison approaches in the entire estimation criteria comprising matched precision, recall, count of exact matches, and positional accurateness. ST-HGM outperforms other three methodologies in whole test images that comprise nearby non-linear intensity alterations, geometric distortions, and many textural variations. The enhanced performance about high matching recall (more compared to 0.5 in matching recall for ST-HGM is given in Fig 2 that consequences in further suitable matches amongst image pairs.

Additionally, ST-HGM employed the affinity tensor-using supersymmetric and probabilistic approach that differentiate true matches amongst the numerous incorrect ones. Therefore, matching the precision and the count of exact matches was more. High positional accuracy was resultant as positional accuracy was primarily defined using the correct matches and matching precision.



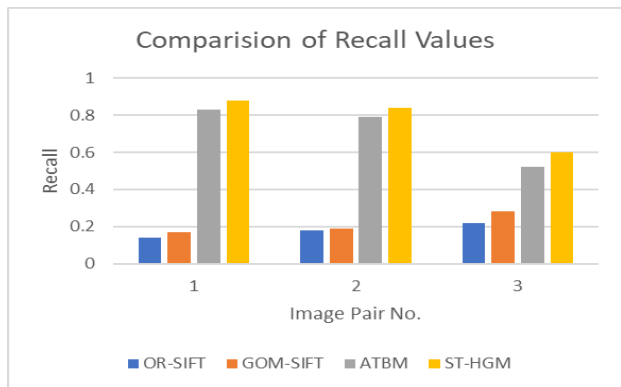


Fig 2: Comparison of Recall Values for the image pairs

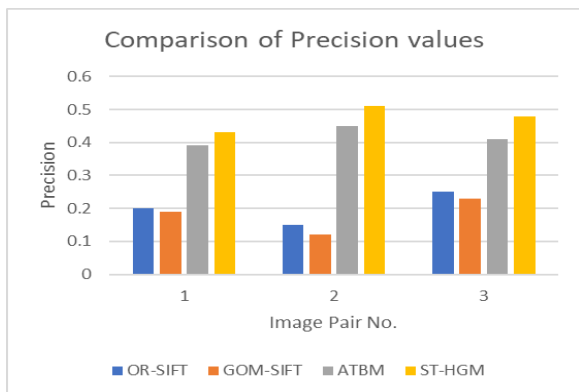


Fig 3: Comparison of Precision Values for the image pairs

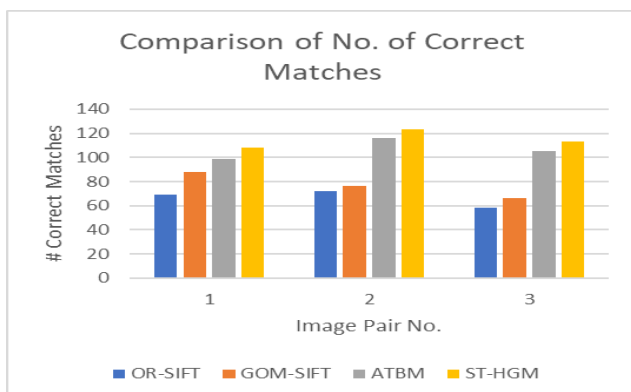
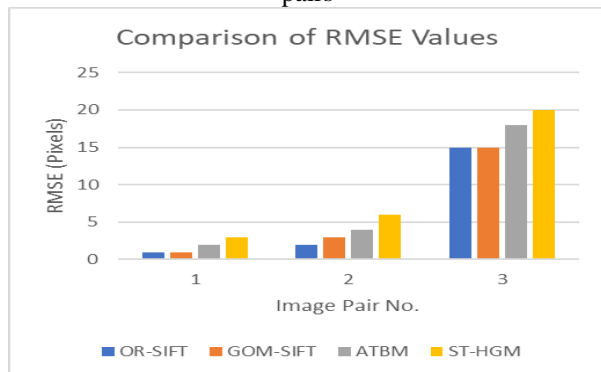


Fig 4: Comparison of No. of correct matches for the image pairs

Fig 5: Comparison of RMSE Values for the image pairs



VI. CONCLUSIONS

An image matching approach is employed in this paper for matching multi-sensor images gathered from different sensors. Initially, for source and target sensor images, the hypergraphs are constructed with third-order pairwise values. Further, the optimal vertex assignment vector is obtained for hypergraph matching using probabilistic affinity tensor evaluation. Also, the supersymmetric is considered where entries are invariant under any permutation of its indices while evaluating the affinity tensor. The proposed approach is experimented on three pairs of sensor image databases and compared with the existing descriptor-based and tensor-based matching algorithm. The experimental outcomes demonstrated that the proposed approach has a higher recall, precision, # accurate matches, and positive accuracy compared to the existing approaches.

REFERENCES

- Z. Lei, J. Longxu, H. Shuangli. Infrared and visible image fusion based on Non subsampledContourlet transform and region classification, *Optics and precision engineering*, 23, 810-818.(2015).
- W. Jianming, J. Zhongliang, W. Zheng. Study on an improved Hausdorff distance for multi-sensor image matching, *Communications in Nonlinear Science & Numerical Simulation*, 17,513-520 (2012)
- W. Yingdan, Y. Ming. A Multi-sensor Remote Sensing Image Matching Method Based on SIFTOperator and CRA Similarity Measure, *ISIE*, 115-118 (2011)
- J. Son, S. Kim, K. Sohn. A Multi-vision Sensor-based Fast Localization System with ImageMatching for Challenging Outdoor Environments, *Expert Systems with Applications*, 42,8830-8839 (2015)
- Y. Luo, S. Juan, M. Qingxun. Multi-sensor Image Matching Method Based on Block ShapeFeatures, *Infrared*, (2013).
- [6] N. Merkle, R. M'uller, and P. Reinartz, "Registration of Optical and SAR Satellite Images Based on Geometric FeatureTemplates," *ISPRS - International Archives of the Photogrammetry, Remote Sensing and Spatial Information Sciences*, vol.XL-1-W5, pp. 447-452, Nov 2015.
- Dellinger, F.; Delon, J.; Gousseau, Y.; Michel, J.; Tupin, F. SAR-SIFT: A SIFT-Like Algorithm for SAR Images. *IEEE Trans. Geosci. Remote Sens.* 2015, 53, 453-466. [CrossRef]
- Ye, Y.; Shen, L.; Hao, M.; Wang, J.; Xu, Z. Robust optical-to-SAR image matching based on shape properties. *IEEE Geosci. Remote Sens.* 2017, 14, 564-568. [CrossRef]
- Ye, Y.; Shen, L. HOPC: A novel similarity metric based on geometric structural properties for multi-model remote sensing image matching. In *Proceedings of the ISPRS Annals of Photogrammetry, Remote Sensing and Spatial Information Sciences*, Prague, Czech Republic, 12-19 July 2016; pp. 9-16.
- Ye, Y.; Shan, J. A local descriptor based registration method for multispectral remote sensing images with non-linear intensity differences. *ISPRS J. Photogramm. Remote Sens.* 2014, 90, 83-95. [CrossRef]
- Shechtman, E.; Irani, M. Matching local self-similarities across images and videos. In *Proceedings of the IEEE Conference on CVPR*, Minneapolis, MN, USA, 17-22 June 2007; pp. 1-8.
- Kovesi, P. Image Features from Phase Congruency. *Video J. Comput. Vis. Res.* 1999, 1, 1-26.
- Kovesi, P. Phase Congruency Detects Corners and Edges. In *Proceedings of the Australian PatternRecognition Society Conference*, Sydney, Australia, 10-12 December 2003; pp. 309-318.
- Sui, H.; Xu, C.; Liu, J.; Hua, F. Automatic optical-to-SAR image registration by iterative line extraction and Voronoi integrated spectral point matching. *IEEE Trans. Geosci. Remote Sens.* 2015, 53, 6058-6072. [CrossRef]
- Shui, P.; Cheng, D. Edge Detector of SAR Images Using Gaussian-Gamma-Shaped Bi-Windows. *IEEE Geosci.Remote Sens.* 2012, 9, 846-850. [CrossRef].



16. Ye, Y.; Shan, J.; Bruzzone, L.; Shen, L. Robust Registration of Multimodal Remote Sensing Images Based on structural Similarity. *IEEE Trans. Geosci. Remote Sens.* 2017, 55, 2941–2958. [CrossRef]
17. Li, J.; Hu, Q.; Ai, M. RIFT: Multi-modal Image Matching Based on Radiation-invariant Feature Transform. *arXiv* 2018, arXiv:1804.09493.
18. Merkle, N.; Luo, W.; Auer, S.; Müller, R.; Urtasun, R. Exploiting Deep Matching and SAR Data for the Geo-Localization Accuracy Improvement of Optical Satellite Images. *Remote Sens.* 2017, 9, 586. [CrossRef]
19. Mou, L.; Schmitt, M.; Wang, Y.; Zhu, X. A CNN for the Identification of Corresponding Patches in SAR and optical Imagery of Urban Scenes. In Proceedings of the 2017 Joint Urban Remote Sensing Event (JURSE), Dubai, UAE, 6–8 March 2017.
20. Hughes, L.H.; Schmitt, M.; Mou, L.; Wang, Y.; Zhu, X.X. Identifying Corresponding Patches in SAR and optical images with a Pseudo-Siamese CNN. *IEEE Geosci. Remote Sens. Lett.* 2018, 15, 784–788. [CrossRef]
21. Dalal, N.; Triggs, B. Histograms of oriented gradients for human detection. In Proceedings of the IEEE Conference on CVPR, San Diego, CA, USA, 20–25 June 2005; pp. 886–893.
22. Xie, H.; Pierce, L.E.; Ulaby, F.T. Statistical Properties of Logarithmically Transformed Speckle. *IEEE Trans. Geosci. Remote Sens.* 2002, 40, 721–727. [CrossRef]
23. Germain, O.; Refregier, P. On the bias of the likelihood ratio edge detector for SAR images. *IEEE Trans. Geosci. Remote Sens.* 2000, 38, 1455–1457. [CrossRef]
24. Schou, J.; Skriver, H.; Nielsen, A.; Conradsen, K. CFAR edge detector for polarimetric SAR images. *IEEE Trans. Geosci. Remote Sens.* 2003, 41, 20–32. [CrossRef]
25. 25. M. Leordeanu, M. Hebert, A spectral technique for correspondence problems using pairwise constraints, in: Proceedings of the IEEE International Conference Computer Vision, 2005, pp. 1482–1489.
26. 26. A. Egozi, Y. Keller, H. Guterman, A probabilistic approach to spectral graph matching, *IEEE Trans. Pattern Anal. Mach. Intell.* 35 (1) (2013) 18–27.
27. 27. R. Sinkhorn, A relationship between arbitrary positive matrices and doubly stochastic matrices, *Ann. Math. Stat.* (1964) 876–879.
28. BalaAnand, M., Karthikeyan, N. & Karthik, S.” Designing a Framework for Communal Software: Based on the Assessment Using Relation Modelling”, *Int J Parallel Prog* (2018). <https://doi.org/10.1007/s10766-018-0598-2>.
29. Venkateswar Lal, P., Nitta, Gnaneshwara Rao. & Prasad, A.,” Ensemble of texture and shape descriptors using support vector machine classification for face recognition” *Journal of Ambient Intelligence and Human Computing*, (2019). <https://doi.org/10.1007/s12652-019-01192-7>.
30. Nitta, Gnaneshwara Rao., Sravani, T., Nitta, S. et al.,” Dominant gray level based k-means algorithm for MRI Images,” *Journal of Health and Technology*, (2019). <https://doi.org/10.1007/s12553-018-00293-1>.
31. Gnaneshwara Rao Nitta, Yogeshwara Rao B Sravani T Ramakrishiah N,” LASSO based Feature Selection and Naïve Bayes classifier for crime prediction and its type,” *Service Oriented Computing and Applications*, Springer, ISSN: 1863-2394, Impact factor:1.40, H-Index:15, (2019).



Dr. N. Sandhya has over 15 years of teaching experience, with research interests in Data mining. She has more than twenty research papers published in reviewed journals. She mentors students every year to improve their technical skills to live up with the market.



Dr. Raghav Mehra has over 13 years of teaching experience and involved in various research activities for more than three years. He has more than 35 papers in his credit which have been published in various international/national journals and refereed conferences. He has taught variety of new subjects and attended variety of workshops and conferences that are relevant to the field of genetic algorithms, software engineering, automated generation of test data, object-oriented systems, object-oriented software testing, evolutionary computing, etc

AUTHORS PROFILE



Mr. Hari kunadharaju is a diligent IT professional with a proven track record of successful delivery in the areas of Application Development and Service Delivery. He is currently working as Vice President @ *Wells Fargo* Enterprise Global Services. He has a Master's degree in Telecommunications Engineering from Monash University, Australia. His research interests include Machine Learning, Data Mining, Data

Warehousing, Cloud Computing, and Software Engineering. He is always focused on achieving the result with a quiet determination, overcoming any obstacles, and exceeds all expectations. He has a strong support experience in the areas of Fixed Income Securities about Global Markets. He has a Machine Learning Certificate from Stanford University. He is a Microsoft SQL Server, Oracle PL/SQL and ITIL (Information Technology Infrastructure Library) Certified Professional.